Influence of Lipid Headgroup on the Specificity and Exchange Dynamics in Lipid–Protein Interactions. A Spin-Label Study of Myelin Proteolipid Apoprotein–Phospholipid Complexes

Laszlo I. Horváth,[‡,§] Peter J. Brophy,[∥] and Derek Marsh*[,‡]

Max-Planck-Institut für biophysikalische Chemie, Abteilung Spektroskopie, D-3400 Göttingen, Federal Republic of Germany, and Department of Biological Science, Stirling University, Stirling FK9 4LA, U.K.

Received November 13, 1987; Revised Manuscript Received February 26, 1988

ABSTRACT: The pH and salt dependences of the interaction of phosphatidic acid, phosphatidylserine, and stearic acid with myelin proteolipid apoprotein (PLP) in dimyristoylphosphatidylcholine (DMPC) recombinants have been studied by electron spin resonance spectroscopy, using spin-labeled lipids. The two-component spin-label spectra have been analyzed both by spectral subtraction and by simulation using the exchange-coupled Bloch equations to give the fraction of lipids motionally restricted by the protein and the rate of lipid exchange between the fluid and motionally restricted lipid populations. For stearic acid, phosphatidic acid, and phosphatidylserine, the fraction of motionally restricted spin-label increases with increasing pH, with pK_a's of 7.7, 7.6, and ca. 9.4, respectively. The corresponding pK_a's for the bulk lipid regions of the bilayer are estimated, from changes in the ESR spectra, to be 6.7, 7.4, and 11, respectively. In the dissociated state at pH 9.0, the fraction of motionally restricted component decreases with increasing salt concentration, reaching an approximately constant value at [NaCl] = 0.5–1.0 M for all three negatively charged lipids. The net decreases for stearic acid and phosphatidic acid are considerably smaller (by ca. 30%) than those obtained on protonating the two lipids, whereas for phosphatidylserine the fraction of motionally restricted lipid in high salt is reduced to that corresponding to phosphatidylcholine. For a fixed lipid/protein ratio, the on-rate for exchange at the lipid–protein interface is independent of the degree of selectivity and has a shallow temperature dependence, as expected for a diffusion-controlled process. The off-rates for exchange, on the other hand, are determined by the selectivity and are in the inverse ratio of the relative association constants. The activation energies associated with the off-rates are considerably larger than for the on-rates and also reflect contributions from the charge on the lipid.

Many intrinsic membrane proteins have been found to be preferentially solvated by negatively charged phospholipids [for a review see Marsh (1985, 1987)]. From spin-label electron spin resonance (ESR)[1] measurements an interesting picture emerges as to the selectivity pattern of membrane proteins for acidic lipids. For example, cytochrome oxidase (Knowles et al., 1981) and the Na,K-ATPase (Esmann et al., 1985) display highest specificity toward cardiolipin, whereas the acetylcholine receptor (Ellena et al., 1983) and the myelin proteolipid apoprotein (Brophy et al., 1984) display a preferential association with free fatty acid and phosphatidic acid. Rhodopsin, on the other hand, exhibits very little selectivity for the different lipid types (Watts et al., 1979; Marsh et al., 1982). This lipid specificity is not in all cases of electrostatic origin since larger changes in specificity are observed on protonation of the charged lipid headgroups than on screening by salt, the difference being ascribed to changes also in hydration (Esmann & Marsh, 1985). It is interesting to note that the effective membrane pK_a's of both phosphatidic and stearic acids lie close to physiological pH, and thus their association with membrane proteins can be changed considerably by small variations in local pH.

The proteolipid apoprotein (PLP), which is the major integral membrane protein of central nervous system myelin (Boggs et al., 1982), can be purified and recombined with dimyristoylphosphatidylcholine (DMPC) in the presence of various spin-labeled lipids (Boggs et al., 1977; Brophy et al., 1984). In the present work we have investigated the lipid specificity of myelin proteolipid apoprotein as a function of headgroup protonation by varying the pH from 6.0 to 9.6 and compared the association of three acidic spin-labeled lipids, phosphatidic acid, stearic acid, and phosphatidylserine, with that of the zwitterionic spin-labeled phosphatidylcholine. The major aim of these experiments is to follow the alterations in selectivity and bulk-to-boundary exchange dynamics occurring on protonation of lipid headgroups at low pH or electrostatic screening at high ionic strength. In addition, the measurements provide a stringent test of the model used previously (Horváth et al., 1988) to calculate the bulk-to-boundary exchange rates and yield further information on the selectivity of the myelin proteolipid apoprotein for negatively charged lipids.

‡ Max-Planck-Institut für biophysikalische Chemie.
§ Permanent address: Institute of Biophysics, Biological Research Centre, Szeged, Hungary.
∥ Stirling University.

[1] Abbreviations: ESR, electron spin resonance; PLP, myelin proteolipid apoprotein; DMPC, 1,2-dimyristoyl-*sn*-glycero-3-phosphocholine; 14-SASL, 14-(4,4-dimethyl-*N*-oxy-2-oxazolidinyl)stearic acid [non-systematic name; systematic names for the spin-labels used in this paper are of the form 2-butyl-4,4-dimethyl-3-oxy-2-oxazolidinetridecanoic acid (and -oyl as a substituent) or 2-butyl-2-(12-carboxydodecyl-4,4-dimethyl-3-oxazolidinyloxy]; 14-PCSL, -PSSL, and -PASL, 1-acyl-2-[14-(4,4-dimethyloxazolidine-*N*-oxyl)stearoyl]-*sn*-glycero-3-phosphocholine, -phosphoserine, and -phosphoric acid; SDS, sodium dodecyl sulfate; EDTA, ethylenediaminetetraacetic acid; Hepes, *N*-(2-hydroxyethyl)piperazine-*N*'-2-ethanesulfonic acid; Tris, tris(hydroxymethyl)-aminomethane; rms, root mean square.

0006-2960/88/0427-5296$01.50/0

Materials and Methods

Materials. Dimyristoylphosphatidylcholine (DMPC) was from Fluka (Buchs, Switzerland). Hepes was from Serva (Heidelberg, FRG). The 14-SASL stearic acid spin-labeled on the C-14 atom position was synthesized according to the methods of Hubbell and McConnell (1971). The corresponding phosphatidylcholine spin-label, 14-PCSL, was prepared as described in Boss et al. (1975). The 14-PASL and 14-PSSL phosphatidic acid and phosphatidylserine spin-labels were prepared from the 14-PCSL label by transphosphatidylation catalyzed by phospholipase D (Comfurius & Zwaal, 1977). Myelin was isolated from bovine spinal cord by the procedure of Benjamins et al. (1976). The proteolipid apoprotein was extracted and delipidated by Sepharose LH-20 chromatography, essentially as described in Brophy (1977). The delipidated preparation contained less than 1 mol of lipid phosphorus/mol of protein. SDS–polyacrylamide gel electrophoresis (Laemmli, 1970) of the delipidated protein revealed bands corresponding to the myelin proteolipid protein (23.5 kDa) and the closely related 20-kDa DM-20 protein, in the ratio of approximately 2–2.5:1. No evidence was found for the presence of the 12-kDa P-12 band in the gels of the delipidated preparation.

Reconstitution. The proteolipid apoprotein was reconstituted with DMPC by dissolving both constituents in 2-chloroethanol and dialyzing exhaustively against three changes of reconstitution buffer (100 mM NaCl, 1 mM EDTA, and 2 mM Hepes, pH 7.4) as previously described (Brophy, 1977). To ensure identical lipid-to-protein ratio, a large batch of dialyzed complex (12 mg of protein/12 mg of DMPC) was always made and divided into several aliquots. The homogeneity of protein incorporation was analyzed by sucrose gradient centrifugation (10–55% sucrose in reconstitution buffer) for 3 h at 40 000 rpm (Beckman SW 40Ti rotor). Samples from the various reconstitutions were recovered as a single band whose position in the gradient was consistent with the lipid-to-protein ratio. Lipid and protein contents were determined by the methods of Eibl and Lands (1969) and Lowry et al. (1951), respectively. The monomer molecular weight of the proteolipid protein was taken as 25 000. In the pH titration experiments each aliquot of the recombinant batch was pelleted and resuspended in 1 mM EDTA and 20 mM phosphate buffer, pH 6.1–9.6 (pH 9.6 was adjusted by titrating with 1 N NaOH). In the salt titration experiments the pellets were resuspended in 1 mM EDTA and 20 mM Tris-HCl buffer, pH 9.0, with a NaCl concentration of 0–2 M.

ESR Spectroscopy. Samples were labeled before dialysis from ethanol solutions of the spin-labeled lipids at a concentration of 15 μg/mg of DMPC; no signal reduction was observed throughout the above sample preparation procedure. The complexes resuspended in the pH/salt buffer series were concentrated by centrifugation (45 min, 90000g), transferred to a 100-μL capillary tube, and pelleted for 15 min at 3000g in a bench centrifuge. ESR spectra were recorded on a Varian E-12 Century Line spectrometer with nitrogen gas flow temperature regulation. Spectra were digitized by using a Digital Equipment Co. LPS system and stored as 1-kword datafiles. Spectral subtractions were performed with interactive graphics, using software written by Dr. W. Möller of this Institute. For details of the ESR spectroscopic methods, see Marsh (1982).

Spectral Simulations. Line-shape calculations allowing for exchange between the two spectral components were performed via the exchange-coupled Bloch equations (McConnell, 1958). Model I of Davoust and Devaux (1982) was used, as applied previously to simulation of the spectra from freely diffusable spin-labels in PLP/DMPC recombinants (Horváth et al., 1988). The basic assumption is that (spin-labeled) lipids can occupy two different kinds of sites, and between any of these two kinds of sites there is a continuous exchange. If M_b and M_f are the magnetizations associated with spin probes in boundary and bulk sites, respectively, then the change of magnetization due to jumping between these two sites is described by the equations

$$dM_b/dt = -\tau_b^{-1}M_b + \tau_f^{-1}M_f \quad (1)$$

and

$$dM_f/dt = \tau_b^{-1}M_b - \tau_f^{-1}M_f \quad (2)$$

where τ_b^{-1} and τ_f^{-1} are the probabilities per unit time of transfer from a protein site to any of the bulk lipid sites and vice versa. τ_b^{-1} and τ_f^{-1} are not necessarily equal; at exchange equilibrium one obtains from eq 1 and 2

$$f\tau_b^{-1} = (1-f)\tau_f^{-1} \quad (3)$$

where f is the fraction of the total magnetization in the boundary component at equilibrium. When eq 1 and 2 are incorporated into the corresponding Bloch equations for M_b and M_f, one obtains an expression for the line shape from which the exchange-coupled two-component spectra can be generated.

The spectral parameters needed for such simulations were adjusted in two stages. First, pure lipid and protein-alone reference spectra were compared with single-component simulated spectra in order to set the principal values of the g- and A-tensors and find the best matching line-width parameters [cf. Horváth et al. (1988)]. The single-component spectra used were recorded at exactly the same temperature as that for the spectrum of the lipid–protein recombinant in question. (This is in contrast to the strategy employed for spectral subtraction, where fluid and motionally restricted components are taken at somewhat lower and higher temperatures, respectively, than those of the recombinant, in order to emulate the effects of exchange.) For all subsequent simulations of two-component spectra corresponding to the same temperature, these parameters for the single components were then held constant. In the second stage, the fraction of motionally restricted component and the exchange frequency were varied independently until the amplitudes of the simulated two-component spectrum (Y_{sim}) matched the line shape of the experimental spectrum (Y_{exptl}). Because this matching is never perfect over the entire spectrum, we introduced an error function

$$(\Delta Y)^2 = \frac{\sum_i (Y_{sim,i} - Y_{exptl,i})^2}{\sum_i (Y_{exptl,i})^2} \quad (4)$$

which has to be minimized by some optimization algorithm. In this work we used a quadratic optimization employed previously (Horváth et al., 1988); the primary advantages of this approach are substantial reductions of computation time and the elimination of subjective criteria in finding the best fit. Each exchange frequency reported below was obtained by this two-stage approach.

It will be noted that two independent parameters are obtained from the exchange simulations. These are the fraction of motionally restricted lipid and one of the two exchange rates, τ_b^{-1} or τ_f^{-1}. The remaining exchange rate is then completely determined by the other two parameters from eq 3. A careful comparison of the values for the fraction of motionally restricted lipid obtained from two-site exchange simulations with those from empirical spectral subtractions showed the two to be in rather good agreement for exchange rates in the range

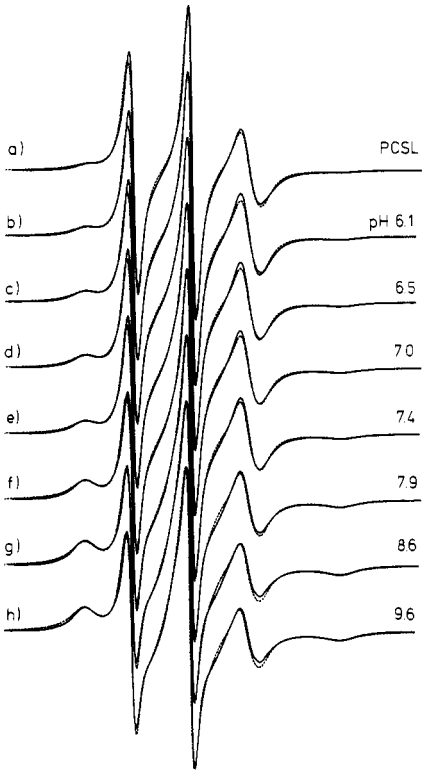

FIGURE 1: ESR spectra of the 14-SASL stearic acid spin-label as a function of pH in myelin proteolipid apoprotein–DMPC recombinants of lipid/protein ratio 37:1 mol/mol: (a) 14-PCSL spin-label at pH 7.4; (b–h) 14-SASL spin-label at the indicated pH values (pH 6.1–9.6). T = 30 °C, scan width = 100 G. Full lines are the experimental spectra, and dotted lines are spectral simulations using the two-component exchange model described in the text. Rms deviations between experimental and simulated spectra are in the range 0.6–0.9%.

normally encountered in lipid–protein systems (Horváth et al., 1988).

Results

pH Dependence. The ESR spectra of the 14-SASL stearic acid spin probe in myelin proteolipid apoprotein–dimyristoylphosphatidylcholine complexes resuspended in 20 mM phosphate buffer at various pH's are shown in Figure 1. The spectra were recorded at 30 °C, which is above the gel-to-fluid phase transition temperature of the host lipid, and so display the fluid and motionally restricted spectral components typical for lipid–protein recombinants. The relative proportion of the motionally restricted component is greater than for phosphatidylcholine, and this lipid selectivity shows a pronounced titration with pH. As was shown previously, the motionally averaged, three-line spectrum of the fluid component is closely similar to that of 14-SASL in DMPC vesicles (Brophy et al., 1984). If the latter pure lipid spectra are digitally subtracted from the two-component recombinant spectra, another spectral component can be identified that otherwise is only apparent at the low-field and high-field parts of the spectra. This broader component well matches the spectrum of 14-SASL in delipidated PLP samples and is therefore assigned to the lipid population occupying solvation sites at the protein interface. From quantitative digital subtractions the relative proportion of the two components can be obtained by using a lipid-alone and protein-alone reference spectrum library. In addition to the results obtained from complementary subtractions, the fractions of motionally restricted component were further verified both by spectral additions (Jost & Griffith, 1978; Brophy et al., 1984) and by pairwise intersubtractions within a given series such as that

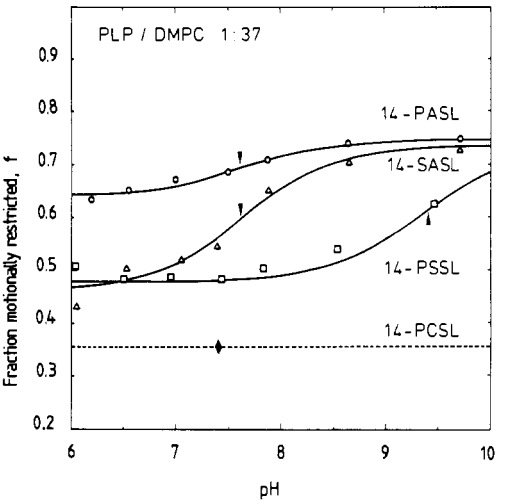

FIGURE 2: pH dependence of the fraction of motionally restricted spin-labels in myelin proteolipid apoprotein–DMPC recombinants of lipid/protein ratio 37:1 mol/mol in 20 mM sodium phosphate buffer: (△) stearic acid spin-label, 14-SASL; (□) phosphatidylserine spin-label, 14-PSSL; (○) phosphatidic acid spin-label, 14-PASL; (◆) phosphatidylcholine spin-label, 14-PCSL. The full curves for 14-SASL, 14-PASL, and 14-PSSL represent least-squares fits to a conventional titration curve: pK_a (14-SASL) = 7.6; pK_a (14-PASL) = 7.6; pK_a (14-PSSL) = 9.4.

shown in Figure 1 (Brotherus et al., 1980; Knowles et al., 1981).

The pH dependences of the mean fraction of motionally restricted component for 14-SASL stearic acid, 14-PASL phosphatidic acid, and 14-PSSL phosphatidylserine in proteolipid apoprotein–dimyristoylphosphatidylcholine complexes of fixed lipid/protein ratio are given in Figure 2. A very clear titration curve is obtained in each case (the 14-PSSL titration being only partial because of the limited pH range) that was fitted to the titration equation

$$f = f_{min} + (f_{max} - f_{min})/(1 + [H^+]/K_a) \qquad (5)$$

where f_{min} and f_{max} are the fractions of motionally restricted component for the protonated and deprotonated forms, respectively, and $pK_a = -\log K_a$. For 14-SASL, 14-PASL, and 14-PSSL the following constants were obtained: f_{min} = 0.46, 0.64, and 0.48; f_{max} = 0.74, 0.75, and 0.74; and pK_a = 7.7, 7.6, and 9.4, respectively. Because 14-PSSL is only partially deprotonated at pH 9.6, the corresponding value for f_{max} was assumed to be identical with that of 14-PASL and 14-SASL. Consequently, the pK_a value for 14-PSSL should be regarded as somewhat approximate.

Parallel titrations of these labels in pure dimyristoylphosphatidylcholine were performed by using the outer hyperfine splitting, A_{max}, as an empirical titration parameter as discussed in Esmann and Marsh (1985). The data for 5-SASL, 5-PASL, and 5-PSSL are given in Figure 3, from which the following pK_a values were obtained: 6.7, 7.4, and 11 (from titrations extending to pH 12), respectively. The 5-PCSL and 14-PCSL phosphatidylcholine spin-labels, on the other hand, displayed no measurable pH dependence. The pK_a values determined from Figures 2 and 3 are identical within experimental uncertainty for phosphatidic acid, whereas the pK_a for phosphatidylserine is one or more pH units higher in the pure lipid than obtained for the lipid–protein interaction, and for stearic acid the reverse is true.

Salt Dependence. The salt dependence of the ESR spectra of the 14-SASL stearic acid spin probe in myelin proteolipid aproprotein–dimyristoylphosphatidylcholine complexes suspended in 20 mM Tris buffer, pH 9.0, is shown in Figure 4.

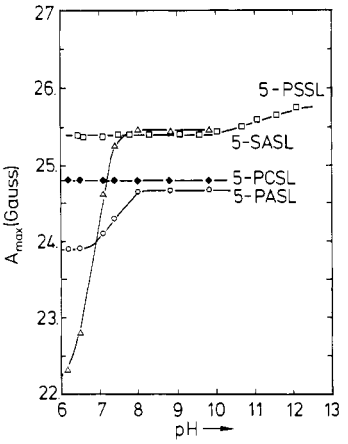

FIGURE 3: pH dependence of the outer hyperfine splitting, A_{max}, for the stearic acid spin-label, 5-SASL (△); the phosphatidic acid spin-label, 5-PASL (○); the phosphatidylserine spin-label, 5-PSSL (□); and the phosphatidylcholine spin-label, 5-PCSL (◆); in DMPC bilayers at 30 °C.

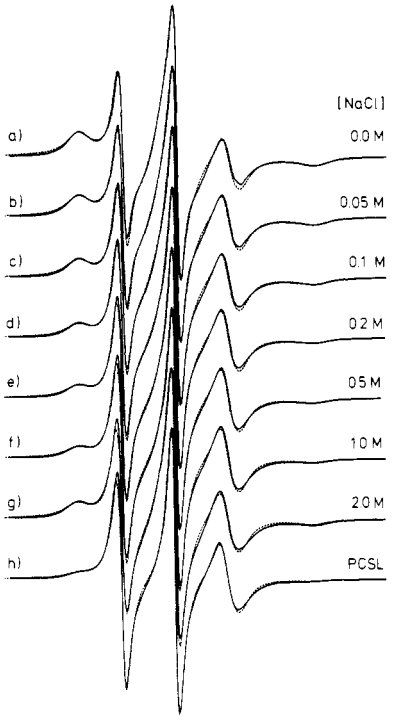

FIGURE 4: ESR spectra of the 14-SASL stearic acid spin-label as a function of NaCl concentration in myelin proteolipid apoprotein–DMPC recombinants of lipid/protein ratio 37:1 mol/mol at pH 9.0: (a–g) 14-SASL spin-label at the indicated NaCl concentrations; (h) 14-PCSL phosphatidylcholine spin-label at 0.1 M NaCl, pH 7.4. T = 30 °C, scan width = 100 G. Full lines are the experimental spectra, and dotted lines are simulations using the two-component exchange model described in the text. Rms deviations between experimental and simulated spectra are in the range 0.6–1.0%.

When the NaCl concentration is increased from <1 mM to 0.1 M, the relative intensity of the motionally restricted component decreases sharply and levels off at a concentration of about 0.5 M, without much further change up to 2 M NaCl. For comparison the ESR spectrum of the 14-PCSL phosphatidylcholine spin probe in a complex from the same batch recorded in the reconstitution buffer is also shown in Figure 4. The 14-PASL phosphatidic acid and the 14-PSSL phosphatidylserine spin probes displayed qualitatively similar salt dependences of their ESR spectra. The quantitative results of these salt titration experiments, in terms of the fraction of motionally restricted component as derived by spectral subtractions and additions, are summarized in Figure 5. It should

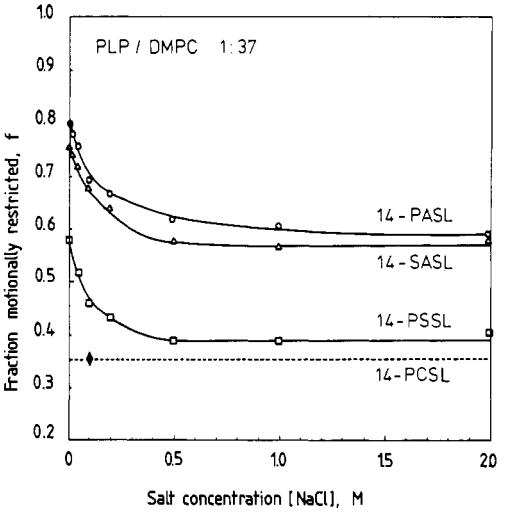

FIGURE 5: Salt dependence of the fraction of motionally restricted lipid spin-label in myelin proteolipid apoprotein–DMPC recombinants of lipid/protein ratio 37:1 mol/mol at pH 9.0: (△) stearic acid spin-label, 14-SASL; (□) phosphatidylserine spin-label, 14-PSSL; (○) phosphatidic acid spin-label, 14-PASL; (◆) phosphatidylcholine spin-label, 14-PCSL.

be noted that for stearic acid, 14-SASL, the limiting value of the fraction of motionally restricted component at high salt concentration is considerably greater than that found for the protonated form at low salt concentration (Figures 2 and 5). For phosphatidic acid, 14-PASL, and phosphatidylserine, 14-PSSL, the fraction of motionally restricted spin-label at high salt concentration is somewhat lower than that obtained at low pH and low salt concentration. In contrast to 14-SASL, however, the latter lipids still bear a net negative charge at pH 6.

Exchange Rates. The effects of the changes in lipid selectivity on the exchange dynamics at the lipid–protein interface can be analyzed by spectral simulation using the exchange-coupled Bloch equations, as outlined under Materials and Methods. The simulated exchange-coupled two-component spectra that best fit the spectra from the pH titration of the 14-SASL stearic acid spin-label are shown by the dotted lines in Figure 1. As can be seen from the figure, the simulations fit the experimental spectra extremely well, with typical root mean square errors between the two lying in the range 0.6–0.9%. The on- and off-rates determined by such simulations are given in Table I for 14-PCSL and for the three acidic spin labels at the different pH's. As expected for a diffusion-controlled on-reaction at fixed lipid/protein ratio, no pH dependence (and certainly no systematic variation) is observed for the on-rates, τ_f^{-1}; all values are reasonably similar for a particular series, including those for 14-PCSL. The off-rates, τ_b^{-1}, on the other hand (which are then determined by the fraction of motionally restricted component, f—see eq 3), exhibit a strong pH dependence and have a titration behavior similar to that of the motionally restricted fraction (cf. Figure 2), with approximately the same pK values. Again the 14-SASL stearic acid spin-label displays the most pronounced pH dependence: in the protonated form the off-rate is approximately half that for phosphatidylcholine, whereas in the deprotonated form it is reduced by a further factor of 3. The 14-PASL phosphatidic acid and the 14-PSSL phosphatidylserine spin-labels display qualitatively similar features, but none of these titration curves are complete in the pH range over which these experiments were performed.

The on- and off-rates obtained from simulating the salt titration spectra (see the dotted lines in Figure 4 for 14-SASL)

Table I: On- and Off-Rate Constants, τ_f^{-1} and τ_b^{-1}, Respectively, for Lipid Exchange of the 14-SASL Stearic Acid, 14-PASL Phosphatidic Acid, 14-PSSL Phosphatidylserine, and 14-PCSL Phosphatidylcholine Spin-Labels at the Lipid–Protein Interface in PLP–DMPC Recombinants as a Function of pH in 10 mM Sodium Phosphate Buffer, T = 30 °C[a]

	14-SASL		14-PASL		14-PSSL	
pH	τ_f^{-1} (s^{-1})	τ_b^{-1} (s^{-1})	τ_f^{-1} (s^{-1})	τ_b^{-1} (s^{-1})	τ_f^{-1} (s^{-1})	τ_b^{-1} (s^{-1})
6.1	6.1×10^6	5.9×10^6	1.1×10^7	4.4×10^6	8.3×10^6	5.3×10^6
6.5	5.5×10^6	4.3×10^6	9.7×10^6	4.2×10^6	7.3×10^6	5.1×10^6
7.0	5.4×10^6	3.8×10^6	1.0×10^7	3.5×10^6	7.5×10^6	5.0×10^6
7.4	5.3×10^6	3.5×10^6	1.0×10^7	3.6×10^6	7.2×10^6	5.2×10^6
7.9	5.7×10^6	2.3×10^6	1.1×10^7	3.6×10^6	7.9×10^6	5.3×10^6
8.6	6.5×10^6	2.1×10^6	1.2×10^7	3.5×10^6	7.4×10^6	4.5×10^6
9.6	6.1×10^6	2.0×10^6	1.1×10^7	3.3×10^6	9.3×10^6	4.4×10^6
7.4 (14-PCSL)	7.9×10^6	1.2×10^7	9.5×10^6	1.1×10^7	7.8×10^6	1.0×10^7

[a] All samples for a given pH series have the same lipid/protein ratio. Data are obtained solely from spectral simulations (see Figure 1) by using a two-component exchange model as described in the text.

Table II: On- and Off-Rate Constants, τ_f^{-1} and τ_b^{-1}, Respectively, for Lipid Exchange of the 14-SASL Stearic Acid, 14-PASL Phosphatidic Acid, 14-PSSL Phosphatidylserine, and 14-PCSL Phosphatidylcholine Spin-Labels at the Lipid–Protein Interface in PLP–DMPC Recombinants as a Function of NaCl Concentration at pH 9.0, T = 30 °C[a]

	14-SASL		14-PASL		14-PSSL	
NaCl (M)	τ_f^{-1} (s^{-1})	τ_b^{-1} (s^{-1})	τ_f^{-1} (s^{-1})	τ_b^{-1} (s^{-1})	τ_f^{-1} (s^{-1})	τ_b^{-1} (s^{-1})
0.0	7.7×10^6	2.2×10^6	1.2×10^7	3.2×10^6	1.3×10^7	5.8×10^6
0.05	8.9×10^6	2.8×10^6	1.1×10^7	3.6×10^6	1.0×10^7	7.5×10^6
0.1	8.5×10^6	3.3×10^6	9.6×10^6	3.9×10^6	9.1×10^6	8.4×10^6
0.2	7.9×10^6	4.5×10^6	9.7×10^6	4.3×10^6	1.0×10^7	1.0×10^7
0.5	8.6×10^6	5.3×10^6	8.6×10^6	5.0×10^6	9.0×10^6	1.1×10^7
1.0	8.9×10^6	6.2×10^6	8.5×10^6	5.2×10^6	8.9×10^6	1.1×10^7
2.0	8.9×10^6	6.0×10^6	9.0×10^6	6.0×10^6	1.0×10^7	1.1×10^7
0 (14-PCSL)	9.9×10^6	1.4×10^7	8.9×10^6	1.5×10^7	1.0×10^7	1.5×10^7

[a] All samples for a given salt concentration series have the same lipid/protein ratio. Data are obtained solely from spectral simulations (see Figure 4) by using a two-component exchange model as described in the text.

are given in Table II. Again the on-rates, τ_f^{-1}, remain reasonably constant, independent of salt concentration, for all three spin probes, although the fraction of motionally restricted component varies considerably over this concentration range. The on-rates for the charged spin probes are also similar to those for phosphatidylcholine, as expected for a diffusion-controlled association at fixed lipid/protein ratio. At low salt concentrations (<0.01 M) the off-rates for the 14-SASL stearic acid, 14-PASL phosphatidic acid, and 14-PSSL phosphatidylserine spin probes differ by factors of 6.4, 4.7, and 2.6, respectively, from those of phosphatidylcholine. As the salt concentration is increased the off-rates also increase and reach a plateau at about 0.5 M concentration, in parallel with the values for the fraction of motionally restricted lipid (cf. Figure 5). However, it should be noted that the off-rates for the 14-SASL stearic acid and 14-PASL phosphatidic acid spin-labels, but not those for the 14-PSSL phosphatidylserine spin-label, remain considerably below that for phosphatidylcholine (by a factor of ca. 2.5), even at the highest salt concentrations.

Temperature Dependence. An Arrhenius plot for the temperature dependence of the off-rates, τ_b^{-1}, for the 14-SASL, 14-PASL, 14-PSSL, and 14-PCSL spin-labels is shown in Figure 6. In the limited temperature interval between the phase transition of DMPC (24 °C) and the high-temperature limit (40 °C) above which protein denaturation can disrupt lipid–protein interactions, each spin probe displays an approximately linear Arrhenius behavior. However, for some labels a somewhat steeper decrease is observed at the lower temperatures, closer to the phase transition, as observed previously for 14-PASL, where the measurements were extended into the phase transition region (Horváth et al., 1988). The 14-PCSL phosphatidylcholine spin-label, which according to previous lipid-to-protein titrations (and the present on/off-rate data) displays no selectivity relative to the host DMPC, has the lowest activation energy: 20 kJ mol^{-1}. 14-SASL and

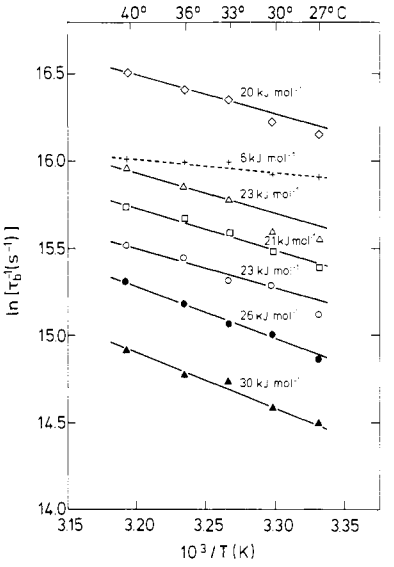

FIGURE 6: Arrhenius plot of the temperature dependence of the exchange off-rate constant, τ_b^{-1}, for the 14-PASL phosphatidic acid (○), 14-SASL stearic acid (△), 14-PSSL phosphatidylserine (□), and 14-PCSL phosphatidylcholine (◇) spin-labels in PLP–DMPC recombinants of fixed lipid/protein ratio. Measurements are at pH 7.4 for 14-PCSL, at pH 6.1 for all other labels, and also at pH 9.7 for 14-$PASL^{2-}$ (●) and 14-$SASL^{-}$ (▲). Activation energies for each spin-label in the different protonation states are shown on the plot. The on-rate constants, τ_f^{-1}, obtained as the means from all spin-labels and at the different pH's are also given (+).

14-PASL in their protonated forms have essentially identical activation energies of 23 kJ mol^{-1}, with 14-PSSL having an activation energy of 21 kJ mol^{-1}. All three activation energies are probably not significantly greater than the value for 14-PCSL. As 14-SASL is titrated to its deprotonated form the activation energy increases to 30 kJ mol^{-1}, and that for 14-PASL increases to 26 kJ mol^{-1} on titrating from its singly to

doubly charged form. The temperature dependence of the on-rate, τ_f^{-1}, is also given in Figure 6. Since there were no appreciably significant differences in on-rates between the different labels or pH's (cf. Tables I and II), the values given are the means for all the different systems. The activation energy associated with the on-rate is rather small, 6 kJ mol^{-1}, much lower than that for any of the off-rates.

Discussion

Two-Component Analysis. The present study builds on previous work by providing new insights into the origin of the specificity of interaction of negatively charged phospholipids with the myelin proteolipid protein (Brophy et al., 1984) and the effects of this specificity on the dynamics of lipid exchange at the lipid–protein interface in this system (Horváth et al., 1988). By changing the pH or salt concentration, it is possible to vary the relative proportions of fluid and motionally restricted lipids, essentially on the same sample without changing either lipid/protein ratio or spin-label. This allows a rather direct test of the methods used to simulate the spectra of the exchange-coupled system, since then any long-range effects of the lipid–protein interaction remain constant as the exchange varies. It is seen from Figures 1 and 4 that an extremely good agreement between simulated and experimental spectra (rms deviations <1%) can be obtained in this way over a wide range of values for the relative proportions of the fluid and motionally restricted components. Hence, these results further demonstrate the validity of the exchange-coupled two-component model generally used for the analysis of the lipid spin-label ESR spectra in natural and reconstituted membranes [cf. Marsh (1985)].

pH Dependence. The results of Figures 2 and 5 show, as found previously for the Na^+,K^+-ATPase (Brotherus et al., 1980; Esmann & Marsh, 1985), that both monovalent salt and pH titration can affect the preferential interaction of negatively charged lipids with the protein. The 14-SASL, 14-PASL, and 14-PSSL spin-labels all show pronounced titration behavior with effective pK_a's for the lipid–protein interaction of 7.6, 7.6, and 9.4, respectively. The effective pK_a can be written as

$$pK_a^{LP} = pK_a^0 + \Delta pK_a^P + \Delta pK_a^{LP} \quad (6)$$

where pK_a^0 is the intrinsic pK_a of the lipid in water, ΔpK_a^P is the pK_a shift due to the lower polarity at the lipid–protein interface, and ΔpK_a^{LP} is the pK_a shift due to the lipid–protein interaction. The polarity shift has been estimated by Fernández and Fromherz (1977) to have the value $\Delta pK_a^P \approx 1.1$ for a micelle surface. At the lipid–protein interface this may be somewhat different. Using values for the intrinsic pK_a from appropriate model compounds [see, e.g., Marsh (1988)], together with the polarity shift, predicts the following interfacial pK_a values: 6.0, 7.6, and 11, for stearic acid, phosphatidic acid, and phosphatidylserine, respectively. These values are reasonably close to those measured in the lipid alone (cf. Figure 3), which provides the reference state for the protein-induced shifts in pK_a. The second shift in eq 6 arises from the preferential selectivity of the protein for one of the two lipid protonation states involved in the acid–base equilibrium. This protein-induced pK_a shift can be related to the relative association constant, K_r, for the lipid (which is introduced below): $\Delta pK_a^{LP} = \log [K_r(LH)/K_r(L^-)]$, where LH and L^- refer to the protonated and deprotonated states of the lipid, respectively. Using the values for the relative association constants of the appropriate species from Table III predicts shifts of $\Delta pK_a^{LP} = -0.2$, -0.5, and -0.5 for 14-PASL, 14-SASL, and 14-PSSL, respectively. The experimental results suggest that the shift is rather small for phosphatidic acid, as predicted. The experimental value of the shift for phosphatidylserine is of the same sign but considerably larger than that predicted. However, it should be noted that the phosphatidylserine titration requires extrapolation (cf. Figure 2) and therefore is subject to some uncertainty. In contrast, it is found that the pK_a shift for stearic acid is large and of the opposite sign to that predicted. Some other interaction, presumably a change in polarity, must outweigh the stabilization of the dissociated form of the fatty acid by the protein. This could be possible because the fatty acid is thought to move vertically in the bilayer on protonation (Barratt & Laggner, 1974).

Table III: Thermodynamic Parameters and Exchange Rate Constants for the Lipid Spin-Label Selectivity in PLP–DMPC Recombinants as a Function of the Lipid Headgroup Protonation and the Ionic Strength (I)[a]

lipid, L	I	τ_b^{-1}(PC)/τ_b^{-1}(L)	K_r^{av}(L)/K_r^{av}(PC)	$\Delta G_L^\circ - \Delta G_{PC}^\circ$[b] (kJ mol^{-1})
PA*$^{2-}$	0.03	3.3	4.7	−3.9
PA*$^{2-}$	2.0	2.5	2.8	−2.6
PA*$^{-}$	0.03	2.5	2.7	−2.5
SA*$^{-}$	0.03	5.8	4.8	−4.0
SA*$^{-}$	2.0	2.3	2.6	−2.4
SA*	0.03	2.0	1.3	−0.6
PS*$^{2-}$	0.03	2.4[c]	3.6[c]	−3.2[c]
PS*$^{2-}$	2.0	1.3[d]	1.4[d]	−0.9[d]
PS*$^{-}$	0.03	2.0	2.7	−2.5
PC*	0.1	1.0	1.0	0.0

[a] Values are derived from the data of Figures 2 and 5 and Tables I and II. T = 30 °C. [b] Derived from values of K_r^{av}(L)/K_r^{av}(PC). [c] Values at pH 9.6, i.e., not fully deprotonated. [d] Values at pH 9.0, i.e., not fully deprotonated.

Analysis of Selectivity. As already mentioned, the selectivity can be analyzed by using the equation for equilibrium association of the spin-labeled lipids with the protein (Brotherus et al., 1981; Knowles et al., 1979)

$$(n_f^*/n_b^*) = n_t/(N_1K_r) - 1/K_r \quad (7)$$

where $(n_f^*/n_b^*) = (1-f)/f$, n_t is the lipid/protein ratio in the recombinant, N_1 is the number of lipid association sites on the protein, and $K_r \approx [L^*P][L]/[L^*][LP]$ is the average association constant of the spin-labeled lipid relative to the background DMPC, defined in terms of moles of lipid. In terms of the true relative association constant K_r^0, defined by activities rather than concentrations

$$K_r = K_r^0(\gamma_{L^*}\gamma_{LP}/\gamma_{L^*P}\gamma_L) \quad (8)$$

where γ_{L^*} and γ_L are the activity coefficients of the labeled and unlabeled lipid, respectively, and γ_{L^*P} and γ_{LP} are similarly defined for the lipid–protein complexes. In previous experiments involving titration of the lipid/protein ratio of PLP–DMPC recombinants, it was demonstrated that the selectivity for the negatively charged lipids arises from an increase in the relative association constant, K_r, rather than in the number of first shell sites, N_1 (Brophy et al., 1984). Thus, for recombinants of a fixed lipid/protein ratio the selectivity relative to a given reference lipid, e.g., 14-PCSL, can be obtained from eq 7 as $(n_f^*/n_b^*)^{PC}/(n_f^*/n_b^*)^L = K_r(L)/K_r(PC)$. These normalized association constants and the differential free energies of association, $\Delta G_L^\circ - \Delta G_{PC}^\circ = -RT \ln [K_r(L)/K_r(PC)]$ derived from them are given in Table III for the spin-labeled lipids in the various charge states and at low and high ionic strength.

It is clear from Table III, and also from Figures 2 and 5, that the selectivity does not depend simply on the net charge of the lipid. The selectivities for $PASL^{2-}$ and $PSSL^{2-}$ are similar to those for $SASL^-$ (at high pH), although the net

charge of the polar groups differs by 1 unit. Analogously, at low pH $PASL^-$ has the same net charge as $PSSL^-$, but there is a very marked difference in the preferential interaction of these two lipids with the protein. Stearic acid in the protonated state (at low pH) also still has a preferential selectivity over phosphatidylcholine, even though neither lipid bears a net charge. The salt dependence provides a means of distinguishing the contribution of the polar group charge to the selectivity, since from Figure 5 it appears that the electrostatic interaction is fully screened at high salt concentration, as might be expected. As seen from Table III and Figures 2 and 5, stearic acid in the charged state at high salt concentration displays a selectivity not only over phosphatidylcholine but also over the uncharged (protonated) form of stearic acid. Phosphatidic acid in its doubly charged form also displays a large selectivity over phosphatidylcholine when electrostatic interactions are fully screened at high salt concentration. In contrast, most of the selectivity displayed by phosphatidylserine can be screened by high salt concentrations. Clearly, electrostatic interactions do play a part in the selectivity of negatively charged lipids for the protein, but for most lipids the detailed chemical nature of the polar headgroup must also have an important role. In addition, the differential screening effects may suggest a heterogeneity of association sites on the protein, with different degrees of accessibility for the various lipids.

Comparison with Na^+,K^+-ATPase. In general, rather similar conclusions have been reached with regard to the selectivity of interaction of spin-labeled phospholipids with the Na^+,K^+-ATPase (Esmann & Marsh, 1985). The results do, however, differ in the details of the interactions of particular lipids with the two proteins. Phosphatidylserine, for instance, shows very little salt dependence and no detectable titration behavior (up to pH 9) in its interaction with the Na^+,K^+-ATPase. Unlike the situation with PLP, phosphatidic acid in its singly charged form and stearic acid in its uncharged form show no preferential association with the Na^+,K^+-ATPase over that observed with phosphatidylcholine. In addition, the preferential interaction of the charged form of stearic acid with the Na^+,K^+-ATPase can be fully screened by salt. Thus, the two proteins display the same qualitative features in the selectivity of their interactions with lipids, but these effects differ in detail and are not necessarily found with the same lipid in each case. The specificity of interaction must, as might be expected, depend on the detailed chemical structure of both lipid and protein.

Exchange Kinetics. The effect of the lipid selectivity on the exchange rates at the lipid–protein interface can be understood in terms of the equilibrium association eq 7, combined with the condition for detailed balance, eq 3. The ratio of exchange rate constants is then given by

$$\tau_b^{-1}/\tau_f^{-1} = n_t/(N_1 K_r) - 1/K_r \qquad (9)$$

It is found from Tables I and II that, for a fixed lipid/protein ratio and a given temperature, the on-rate is constant independent of the lipid headgroup or degree of selectivity. This result is to be expected if the on-rate is diffusion-controlled [as assumed previously (Horváth et al., 1988)] and gives further support to the method used for the spectral simulations. Previous experiments, measuring the collision rates between diffusable ^{14}N-labeled lipids and ^{15}N-labeled chains covalently linked to the protein, have demonstrated directly that the on-rate for the interaction of different phospholipids with the intramembranous surface of rhodopsin is also diffusion-controlled, as expected (Davoust et al., 1983). ESR experiments on the spin–spin broadening of interacting spin-labels have also shown that the lateral diffusion rates in protein-free DMPC bilayers at 30 °C are not strongly dependent on the lipid headgroup type (J.-H. Sachse and D. Marsh, unpublished results).

Since the on-rates can be assumed to remain constant for different lipid spin-labels, say L and PC, then at a fixed lipid/protein ratio and fixed temperature, the ratio of off-rate constants from eq 9 is

$$\tau_b^{-1}(\mathrm{PC})/\tau_b^{-1}(\mathrm{L}) = K_r(\mathrm{L})/K_r(\mathrm{PC}) \qquad (10)$$

This relation is found to hold reasonably well for both the pH and ionic strength dependence of the off-rates for all three acidic spin labels, as shown in Table III. Some discrepancies are found at the higher selectivities for which small changes in the fraction of motionally restricted lipid can produce rather large changes in the ratios. However, the overall agreement demonstrates rather well the effect of selectivity in retarding the lipid off-rates.

Even in the absence of selectivity, the off-rates for, say, PC exchange are appreciably slower than those for lateral diffusion in protein-free bilayers. In DMPC bilayers at 30 °C, the latter have been determined to be (cf. Tables I and II) $\tau_{dif}^{-1} = 4D_T/\langle x^2\rangle \sim 3.7 \times 10^7\ s^{-1}$ by photobleaching (Vaz et al., 1985) and $7.5 \times 10^7\ s^{-1}$ for spin-labeled phosphatidylcholine by ESR spectroscopy (Sachse et al., 1987). As pointed out previously (Horváth et al., 1988), this corresponds to an effective association constant of $K_{eff}^{av} \sim 2$–5 for the lipid–protein interaction referred relative to the lipid–lipid interaction.

Salt Dependence. The salt dependence of the selectivity can be interpreted, at least semiquantitatively, by using the Debye–Hückel theory of electrolytes (Esmann & Marsh, 1985). The activity coefficients of the various charged species involved in eq 8 are given by

$$\ln \gamma_i = \frac{-Z_i^2 e^2}{8\pi\epsilon_0\epsilon kT}\,\frac{\kappa}{1+\kappa a_i} \qquad (11)$$

where Z_i is the charge on species i, a_i is the effective interaction distance of species i with counterions, and the inverse Debye screening length is $\kappa = (2000 N_A e^2 I/\epsilon_0\epsilon kT)^{1/2}$, I being the ionic strength of the electrolyte. Hence, the ratio of relative association constants in the presence and absence of salt is given by

$$\ln (K_r/K_r^0) = \frac{-e^2\kappa}{8\pi\epsilon_0\epsilon kT}\left[\frac{Z_{L^*}^2}{1+\kappa a_{L^*}} + \frac{Z_P^2}{1+\kappa a_P} - \frac{(Z_P + Z_{L^*})^2}{1+\kappa a_{L^*P}}\right] \qquad (12)$$

where L*, P, and L*P represent the lipid spin-label, the protein, and the lipid–protein complex, respectively. If it is assumed for simplicity that the charge on the lipid and the net charge on the protein approximately cancel (i.e., $Z_P = +1$ or $+2$, where appropriate), the last term on the right in eq 12 may then be neglected. An effective value for the protein radius can be taken to be $a_P = 1.65$ nm, in agreement with estimates from the protein molecular weight and partial specific volume (Curatolo et al., 1977); this value is also in agreement with our lipid–protein titration data (Brophy et al., 1984). The effective lipid interaction radius, a_L, can then be treated as an adjustable parameter such that the Debye–Hückel theory can be extended to fit the screening behavior at high electrolyte concentrations [cf. Robinson and Stokes (1955)].

Experimentally, the ratio of the relative association constants in the presence and absence of salt, $K_r(\mathrm{NaCl})/K_r(0)$, can be obtained either from the fraction of motionally restricted lipid or from the exchange rates by using eq 7 or 9, respectively. Consistent values are obtained from both methods, and the

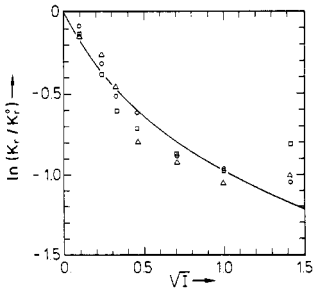

FIGURE 7: Ionic strength (I) dependence of the relative association constant of 14-SASL stearic acid (△), 14-PASL phosphatidic acid (○), and 14-PSSL phosphatidylserine (□) in PLP–DMPC recombinants of fixed lipid/protein ratio. Experimental points are the means of the values deduced from the fraction of motionally restricted lipid and from the exchange rate. The theoretical curve is obtained from Debye–Hückel theory according to eq 12 with $Z_L = -1$, $a_L = 0.15$ nm, and $a_P = 1.65$ nm. The values of the relative association constant, K_r, are normalized to the value at zero ionic strength, K_r^0. For the experimental points, K_r^0 is obtained by extrapolation of the approximately linear dependence of K_r on $I^{1/2}$ at low ionic strength.

means of the resulting ratios are given in Figure 7. Very similar normalized values are obtained for all three lipids, with perhaps a slightly steeper screening for stearic acid. The salt dependence for all three labels can be fitted reasonably well by taking values of $a_L = 0.15$ nm, with $a_P = 1.65$ nm and $Z_L = -1$. This value of a_L is somewhat smaller than that previously used for stearic acid in Na,K-ATPase membranes (Esmann & Marsh, 1985) and rather similar to that used for cardiolipin interacting with cytochrome oxidase (Powell et al., 1987). It should be noted, however, that $Z_L = -1$ is half that appropriate for phosphatidic acid at pH 9.2. Taking $Z_{PA} = -2$, on the other hand, requires an extremely large value of the effective interaction diameter $a_{PA} = 4.0$ nm, as noted previously in connection with the Na,K-ATPase (Esmann & Marsh, 1985).

Activation Energies. Electrostatic interactions will also contribute to the activation energy for exchange (cf. Figure 6). For instance, the activation energy for the charged form of stearic acid is 7 kJ mol^{-1} greater than for the uncharged form; the activation energy for the singly charged form of phosphatidic acid is 3 kJ mol^{-1} and for the doubly charged form 6 kJ mol^{-1} greater than that for the uncharged phosphatidylcholine. For phosphatidylserine, on the other hand, the activation energy is very similar to that for phosphatidylcholine. In principle, the size of the electrostatic effect can be estimated from an extension of Debye–Hückel theory. The additional contribution to the activation energy is given by (Debye, 1943)

$$\Delta E_a = \left[\frac{N_A Z_P Z_L e^2}{2\epsilon}\right]\left[\frac{e^{-\kappa(r_P + r_L)}f}{r_P + r_L}\right]\left[\frac{e^{\kappa r_P}}{1 + \kappa r_P} + \frac{e^{\kappa r_L}}{1 + \kappa r_L}\right] \quad (13)$$

where r_P is the protein radius and r_L is the lipid radius. Using values of $r_P = 1.65$ nm and $r_L = 0.15$ nm gives a value of $\Delta E_a = 4.2$ kJ mol^{-1} for an ionic strength of $I = 0.05$. This is comparable in size to the effects seen with stearic acid and phosphatidic acid. For $r_L = 0.5$ nm, $\Delta E_a = 2.8$ kJ mol^{-1} at $I = 0.05$, corresponding to the rather small effect seen with phosphatidylserine.

Summary. The interaction of phosphatidic acid, stearic acid, and phosphatidylserine with the myelin proteolipid protein responds both to pH titration and ionic screening by salt. For phosphatidic acid and stearic acid, the selectivity of interaction is only partially electrostatic in nature, whereas for phosphatidylserine it can be almost completely screened by salt. The thermodynamics of the interaction are reflected directly in the kinetics of the lipid exchange at the protein interface. The on-rate for the latter is shown to be diffusion-controlled, whereas the off-rates reflect the lipid selectivity. The pH and salt dependences of the exchange at a fixed lipid/protein ratio provide a convincing demonstration of the adequacy of the model used to describe the exchange kinetics and of the two-component analysis used in the interpretation of the spin-label ESR spectra in lipid–protein systems.

ACKNOWLEDGMENTS

We thank S. Chatterjee for her skillful technical assistance in preparing the protein.

Registry No. DMPC, 18194-24-6; stearic acid, 57-11-4.

REFERENCES

Barratt, M. D., & Laggner, P. (1974) *Biochim. Biophys. Acta 363*, 127–133.

Benjamins, J. A., Miller, S. L., & Morell, P. (1976) *J. Neurochem. 27*, 565–570.

Boggs, J. M., Wood, D. D., Moscarello, M. A., & Papahadjopoulos, D. (1977) *Biochemistry 16*, 2325–2329.

Boggs, J. M., Moscarello, M. A., & Papahadjopoulos, D. (1982) in *Lipid–Protein Interactions* (Jost, P. C., & Griffith, O. H., Eds.) Vol. 2, pp 1–51, Wiley-Interscience, New York.

Boss, W. F., Kelley, C. J., & Landsberger, F. R. (1975) *Anal. Biochem. 64*, 289–292.

Brophy, P. J. (1977) *FEBS Lett. 84*, 92–95.

Brophy, P. J., Horváth, L. I., & Marsh, D. (1984) *Biochemistry 23*, 860–865.

Brotherus, J. R., Jost, P. C., Griffith, O. H., Keana, J. F. W., & Hokin, L. E. (1980) *Proc. Natl. Acad. Sci. U.S.A. 77*, 272–276.

Brotherus, J. R., Griffith, O. H., Brotherus, M. O., Jost, P. C., Silvius, J. R., & Hokin, L. E. (1981) *Biochemistry 20*, 5261–5267.

Comfurius, P., & Zwaal, R. F. A. (1977) *Biochim. Biophys. Acta 488*, 36–42.

Curatolo, W., Sakura, J. D., Small, D. M., & Shipley, G. G. (1977) *Biochemistry 16*, 2313–2319.

Davoust, J., & Devaux, P. F. (1982) *J. Magn. Reson. 48*, 475–494.

Davoust, J., Seigneuret, M., Hervé, P., & Devaux, P. F. (1983) *Biochemistry 22*, 3146–3151.

Debye, P. (1943) *Trans. Electrochem. Soc. 82*, 265–272.

Eibl, H., & Lands, W. E. M. (1969) *Anal. Biochem. 30*, 51–57.

Ellena, J. F., Blazing, M. A., & McNamee, M. G. (1983) *Biochemistry 22*, 5523–5535.

Esmann, M., & Marsh, D. (1985) *Biochemistry 24*, 3572–3578.

Esmann, M., Watts, A., & Marsh, D. (1985) *Biochemistry 24*, 1386–1393.

Fernández, M. S., & Fromherz, P. (1977) *J. Phys. Chem. 81*, 1755–1761.

Horváth, L. I., Brophy, P. J., & Marsh, D. (1988) *Biochemistry 27*, 46–52.

Hubbell, W. L., & McConnell, H. M. (1971) *J. Am. Chem. Soc. 93*, 314–326.

Jost, P. C., & Griffith, O. H. (1978) in *Molecular Specialization and Symmetry in Membrane Function* (Solomon, A. K., & Karnovsky, M., Eds.) pp 31–60, Harvard University, Cambridge, MA.

Knowles, P. F., Watts, A., & Marsh, D. (1979) *Biochemistry 18*, 4480–4487.

Knowles, P. F., Watts, A., & Marsh, D. (1981) *Biochemistry 20*, 5888-5894.
Laemmli, U. K. (1970) *Nature (London) 227*, 680-685.
Lowry, O. H., Rosebrough, N. J., Farr, L., & Randall, R. J. (1951) *J. Biol. Chem. 193*, 265-275.
Marsh, D. (1982) *Tech. Life Sci.: Biochem. B4*, B426/1-B426/44.
Marsh, D. (1985) in *Progress in Protein-Lipid Interactions* (Watts, A., & De Pont, J. J. H. H. M., Eds.) Vol. 1, pp 143-172, Elsevier, Amsterdam.
Marsh, D. (1987) *J. Bioenerg. Biomembr. 19*, 677-689.
Marsh, D. (1988) *Handbook of Lipid Bilayers*, CRC, Boca Raton, FL.
Marsh, D., Watts, A., Pates, R. D., Uhl, R., Knowles, P. F., & Esmann, M. (1982) *Biophys. J. 37*, 265-274.
McConnell, H. M. (1958) *J. Chem. Phys. 28*, 430-431.
Powell, G. L., Knowles, P. F., & Marsh, D. (1987) *Biochemistry 26*, 8138-8145.
Robinson, R. A., & Stokes, R. H. (1955) *Electrolyte Solutions*, Butterworths, London.
Sachse, J.-H., King, M. D., & Marsh, D. (1987) *J. Magn. Reson. 71*, 385-404.
Vaz, W. L. C., Clegg, R. M., & Hallmann, D. (1985) *Biochemistry 24*, 781-786.
Watts, A., Volotovski, I. D., & Marsh, D. (1979) *Biochemistry 18*, 5006-5013.

Spin-Label and Fluorescence Labeling Studies of the Thioester Bonds in Human α_2-Macroglobulin†

Baolu Zhao,‡ Giovanni Musci,§ Yoshiaki Sugawara,‖ and Lawrence J. Berliner*
Department of Chemistry, The Ohio State University, Columbus, Ohio 43210
Received August 31, 1987; Revised Manuscript Received January 11, 1988

ABSTRACT: Upon cleavage of the reactive thioester bonds (Cys-949-Glx-952) of tetrameric human α_2-macroglobulin (α_2M) by methylamine, one sulfhydryl group per α_2M subunit is exposed. These identical sulfhydryl group sites were labeled with the thiol-specific nitroxide spin-labels (1-oxy-2,2,5,5-tetramethyl-3-pyrrolin-3-yl)methyl methanethiosulfonate and (1-oxy-2,2,6,6-tetramethyl-4-piperidinyl)methyl methanethiosulfonate, a homologous series of maleimide spin-labels, and the thiol-specific fluorescent probe 2-[(4-maleimidophenyl)amino]naphthalene-6-sulfonic acid sodium salt (MANS). The ESR and fluorescence results showed that these sulfhydryl group sites were at the base of a narrow crevice that is ≥8 Å deep. Although the bound MANS fluorophore was slightly blue shifted with an enhanced quantum yield vs the free label in water, the environment of the sulfhydryl site appeared to be of a polar nature when compared with the emission maxima in several solvents of varying polarity. The Glx residue participating in the thioester linkage in the intact protein was labeled with 4-amino-2,2,6,6-tetramethylpiperidine-1-oxyl. The distance between the Glx and Cys moieties was estimated at ≥10-25 Å from double spin-labeling experiments.

The plasma protein α_2-macroglobulin (α_2M)[1] has a series of unique biochemical properties (Harpel & Brower, 1983). It is a M_r 725 000 glycoprotein composed of two noncovalent bound dimers, each of which contains two identical "subunits" linked together by disulfide bridges (Jones et al., 1972). Each subunit contains 1451 amino acid residues with 8 asparagine-linked oligosaccharide groups (Sottrup-Jensen et al., 1984). Of most interest, however, is the occurrence in each subunit of a labile peptide bond in the "bait region" that is cleaved upon interaction with serine proteinases (Harpel, 1973; Swenson & Howard, 1979). Upon covalent incorporation of methylamine at a thioester linkage about 240 residues away (Glx-952) resulting in the exposure of one sulfhydryl group (Cys-949) per subunit, a conformational change of the whole tetramer occurs which closely mimics that which occurs upon cleavage of the bait region (Larsson et al., 1985; Eccleston & Howard, 1985). The thioester sites are also in close proximity to the proteinase binding sites (Pochon et al., 1981; Feldman et al., 1985). This inhibition mechanism has been proposed to occur via a "trap" mechanism (Barrett & Starkey, 1973; Van Leuven, 1982), which appears to be unique among proteinase inhibitors. That is, a limited proteolysis in the bait region of an α_2M subunit is followed by a conformational change, during which the reactive thioester bonds are cleaved.

Several thiol-specific nitroxide spin-labels have been synthesized that bind covalently to cysteine residues, resulting in

† This work was supported in part by a grant from the USPHS (HL 24549).
* To whom correspondence should be addressed.
‡ On leave from the Institute of Biophysics, Academia Sinica, Beijing, China.
§ Permanent address: Department of Biochemical Sciences, University of Rome, La Sapienza, Piazzale Aldo Moro, 5, Rome, Italy.
‖ Present address: Department of Physiology, Hiroshima Women's University, Hiroshima, Japan.

[1] Abbreviations: α_2M, α_2-macroglobulin; CPK, Corey-Pauling-Koltun; DTNB, 5,5'-dithiobis(2-nitrobenzoic acid); ESR, electron spin resonance; 4-amino-TEMPO, 4-amino-2,2,6,6-tetramethylpiperidine-1-oxyl; Hepes, *N*-(2-hydroxyethyl)piperazine-*N*'-2-ethanesulfonic acid; MANS, 2-[(4-maleimidophenyl)amino]naphthalene-6-sulfonic acid sodium salt; maleimide spin-label **1**, 4-maleimido-TEMPO; maleimide spin-label **2**, 3-(maleimidomethyl)proxyl; maleimide spin-label **3**, 3-[(2-maleimidoethyl)carbamoyl]proxyl; maleimide spin-label **4**, 3-[(3-maleimidopropyl)carbamoyl]proxyl; maleimide spin-label **5** 3-[[2-(2-maleimidoethoxy)ethyl]carbamoyl]proxyl; piperidine thiol spin-label, (1-oxy-2,2,6,6-tetramethyl-4-piperidinyl)methyl methanethiosulfonate; proxyl, 2,2,5,5-tetramethylpyrrolidine-1-oxyl; proxyl thiol spin-label, (1-oxy-2,2,5,5-tetramethyl-3-pyrrolin-3-yl)methyl methanethiosulfonate; STI, soybean trypsin inhibitor; Tos-Arg-OMe, *p*-tosylarginine methyl ester; SDS-PAGE, sodium dodecyl sulfate-polyacrylamide gel electrophoresis.

0006-2960/88/0427-5304$01.50/0